Phase Diagrams of Aqueous Solutions of Polycarboxylates in the Presence of Divalent Cations

Monique A. V. Axelos

Laboratoire de Physicochimie des Macromolécules, INRA La Géraudière,
44026 Nantes Cedex 03, France

Michèle M. Mestdagh

Unité de Chimie des Interfaces, Place Croix du Sud 2/18, 1348 Louvain-La-Neuve, Belgium

Jeanne Francois*

Institut Charles Sadron CNRS, Université Louis Pasteur,
6 rue Boussingault, 67083 Strasbourg Cedex, France

Received March 7, 1994; Revised Manuscript Received July 26, 1994®

ABSTRACT: Phase separation and gelation phenomena induced by addition of divalent cations in aqueous solutions of synthetic and natural polycarboxylates have been investigated by comparison of their phase diagrams. Three major types of behavior may be identified on the basis of the position and shape of the demixing line in the phase diagram, regardless of the chemical structure of the polymer. We propose a model for quantitative prediction of the demixing and sol–gel transition. The relevant parameters introduced are the neutral units, the charge density, and the cation/polyanion affinity, all of which are responsible for inter- and intramolecular complexes. Besides this general scheme, the local configuration of the backbone in natural polymers seems to promote intermolecular cross-links, leading to a large gel phase.

Introduction

Numerous applications of synthetic and biological polyelectrolytes are based upon the control of their interactions with multivalent ions. For instance, in oil recovery processes, copolymers of acrylamide and acrylic acid are used as thickening agents; ions such as Ca^{2+}, Fe^{3+}, or Al^{3+} lead to precipitation and gelation which must be taken into account in order to avoid plugging of the porous media. Other processes take advantage of this aggregation and gelation phenomena; in particular, in food industry, in recovery of heavy metal ions in depollution treatment of waste waters, etc.

The ion–polymer interactions are often described in terms of the Manning[1,2] or Iwasa[3] theories which predict ionic condensation when the charge density of the polymer exceeds a critical value. These approaches have been successfully used[4–9] to explain the behavior of polyelectrolytes in the presence of monovalent cations but fail when multivalent ions and polycarboxylates are concerned.[4–12] Some discrepancies between predictions and results have been reported even in certain cases of monovalent ions.[13] These theories do not take into account the specific interactions (complexation) that are directly related to the nature of the counterions and interactions of the ionic groups on the polymer. Besides, they consider the polymer as a uniformly charged line and neglect the effects of the charge distribution along the chain.

A more phenomenological approach[14] consists of expressing the interactions in terms of multi-equilibrium complexation. This gives a good account of the experimental binding isotherms and reflects the specific effects that are neglected in the Manning theory. The more elaborate theory of Gueron and Weisbuch[15,16] introduces into the equilibrium expression the real concentration of the counterions in the immediate vicinity of the polyions calculated through a numerical solution of the Poisson–Boltzmann equation. Nevertheless, no theory is able to predict the threshold of precipitation and the sol–gel transition.

The phase separation of synthetic polymers has been extensively investigated by several authors (poly(acrylic acid)[17–21] (PAA), poly(methacrylic acid)[22] (PMA), polyphosphate,[23] sulfonated polystyrene and polyethylene[24–27]). A set of experimental studies of the stability of PAA solutions in the presence of alkaline earth cations as a function of pH led Ikegami and Imai[20] to consider two types of phase separation.

(1) **In type H,** a high salt concentration is required to induce the polymer precipitation. The critical salt concentration $[M^{n+}]^*$ at the phase separation is independent of the polymer concentration C_p and is an increasing function of temperature. This behavior is well explained by Flory's model[28] which takes into account the decrease of the electrostatic part of the free energy with the ionic strength I.

(2) **In type L,** precipitation is observed at low values of $[M^{n+}]^*$, in stoichiometric proportion with respect to the number of charged groups of the polymer.

These two types of phase separation describe extreme behaviors. The H type is observed when specific interactions between ions and polyions can be neglected: in the case of very weakly charged polyelectrolytes in the presence of divalent cations (for example PAA at low pH with Ca^{2+}) or strongly charged polyelectrolytes in the presence of monovalent cations (PAA at pH 5 with Na). The L type describes the behavior of strongly charged polymers which interact in a specific manner with counterions (PAA with Ca^{2+}, Ba^{2+}, etc.).

In fact, a wide range of behavior can be observed according to the charge density of the polyion, pH, ionic strength, and the nature of the cationic species. Moreover, gelation is not considered in such a description. Considerable effort has been recently made to establish the phase diagrams including regions of transparent solutions, homogeneous gels, and the two-phase equilibria, for a number of mixtures obtained with various polycarboxyl-

---

* To whom correspondence should be addressed.

® Abstract published in *Advance ACS Abstracts*, September 1, 1994.

0024-9297/94/2227-6594$04.50/0 © 1994 American Chemical Society

ates of synthetic[29-37] and natural[38,39] origin, in the presence of multivalent cations.

This paper discusses the variations of the limits of phase separation and gelation as a function of pertinent parameters through the comparison of different phase diagrams. Acrylic acid–acrylamide copolymers on one hand, alginates and pectins on the other hand, are selected as examples of synthetic and natural polycarboxylates, respectively. The average number of charges and/or their distribution can be changed for all these polymers. Moreover, the physicochemical and conformational properties in the absence of multivalent ions are well-known in the dilute and semidilute regimes.[36,39-50] These two polymer families differ strongly in regard to the flexibility of their chemical bonds and to the length of their monomeric unit. Hence their comparison allows us to test how such characteristics which play an important role in the local structure of cation–carboxylate complexes influence the macroscopic behavior. We show that the behavior of these polymers in the presence of various cations, Ca^{2+}, Mn^{2+}, and Cu^{2+} exhibit the same tendencies and can be interpreted through the same general scheme of interactions with affinity constants depending on the characteristics of each macromolecular chain and on the electronic configuration of the ions.

Polymers

Polyelectrolytes are characterized by the average dimensionless charge density parameter, ξ, given by[1]

$$\xi = (e^2/\epsilon kT)/b \tag{1}$$

where the numerator is the Bjerrum length (7.14 Å in water at 25 °C) and b is the average spacing between two charges, assuming a statistical distribution of the charges. In the specification of this parameter, it is assumed that the chain exists at its maximum expansion and that the effective dielectric constant is that of bulk water.[51] Both these assumptions seem to be unrealistic; the effective dielectric constant, in the vivinity of organic acids is much lower than the bulk value of water.[52,53] Nevertheless, we have used this parameter as usually defined.

The acrylamide–acrylic acid copolymers (PAM) are characterized by τ, the molar fraction of acrylic acid. They can be prepared either by direct copolymerization of the two monomers (AD series) or by alkaline hydrolysis of polyacrylamide (H series). These methods are known to result in different distributions of the monomers along the chain. The diagrams discussed here were obtained with copolymers exhibiting a quasi Bernouillan distribution and with hydrolysis products in which the carboxylate groups tend to be isolated along the chain, as already described.[44,45] For these polymers, $\xi = 2.89\tau\alpha$, where α is the ionization degree of carboxylate groups, which depends on pH, C_p, and I.[42,43] Under the experimental conditions used here, ξ varies between 0.04 and 1.2. The molecular weight of these polymers is about 5×10^6 with a polydispersity index around 2.

Pectins (PEC series) are anionic polysaccharides extracted from the primary plant cell wall. They consist of a linear backbone of randomly α(1–4) linked D-galacturonic acid units and their methyl esters,[54] as shown below:

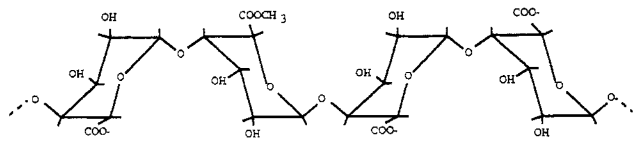

The variation of the number and distribution of the methyl-esterified carboxyl groups along the backbone, obtained by acid deesterification of a high-methoxyl pectin,[38] allows us to vary ξ between 0.44 and 1.16 with the molar fraction of galacturonic acid units τ between 0.27 and 0.73, at $\alpha = 1$. The charge distribution is random, and the molecular weight ranges from 1.6×10^5 to 2×10^5 with a polydispersity index around 3.

Alginates, extracted from brown alga, are linear, binary copolymers of α(1–4) linked α-L-guluronic acid (G) and its C-5 epimer, β-D-mannuronic acid (M) residues:[55]

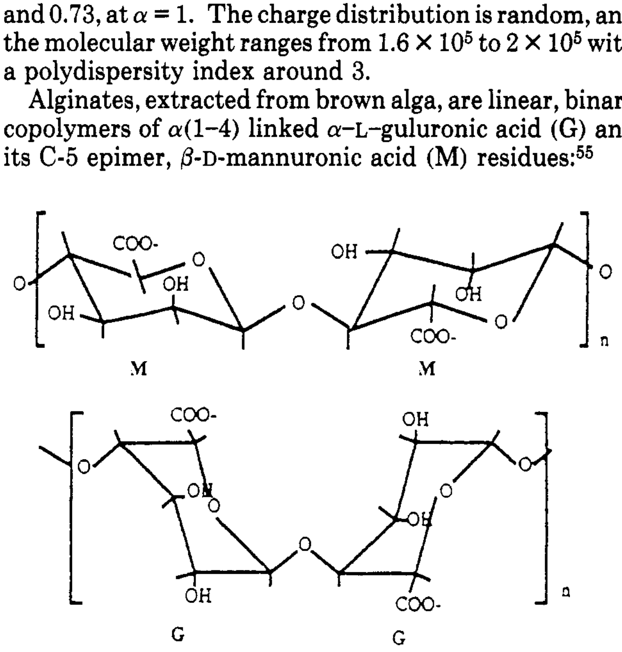

Their properties vary as a function of the ratio x = G/M and the distribution of the monomeric units in the chain. They are arranged in a blockwise pattern along the backbone with homopolymeric regions of M or G types, interspaced with sequences containing both monomers. The proportion and sequential arrangement of the uronic acids depend on the source. Here ξ depends on the ratio G/M, according to

$$\xi = 7.13\alpha \frac{x + 1}{b_G + x b_M} \tag{2}$$

where b_G and b_M are the lengths of the guluronic (4.35 Å) and mannuronic (5.2 Å) units, respectively.[56] The weight average molecular weight of the alginate investigated, obtained from the intrinsic viscosity,[57] is 7×10^5, and x = 0.16, as determined by a polarimetric method.[58]

Phase Diagrams

The phase diagrams were obtained according to the following procedure. The polymer samples were dissolved in pure water or in NaCl aqueous solutions, at their own pH. The pH was adjusted to the required value by addition of solutions of hydrochloric acid or sodium hydroxide. The salt solutions were also prepared at their own pH and if necessary adjusted to the same pH as those of the polymer solutions. Equal volumes of polymer and salt solutions were mixed and vigorously stirred. In all cases, the experimental conditions were chosen in order to minimize the change of pH.

The range of polymer concentration investigated was between 0.01 and 20 g/L. Phase diagrams were established by plotting the molar concentration of cations added [M^{n+}] against the polymer concentration C_p (in g/L). We report here only the results obtained on equilibrated systems at room temperature.

Figure 1 is a schematic representation of the phase diagrams obtained with these systems. The diagrams always contain two main regions separated by the demixing curve. Below this line, only a homogeneous and transpar-

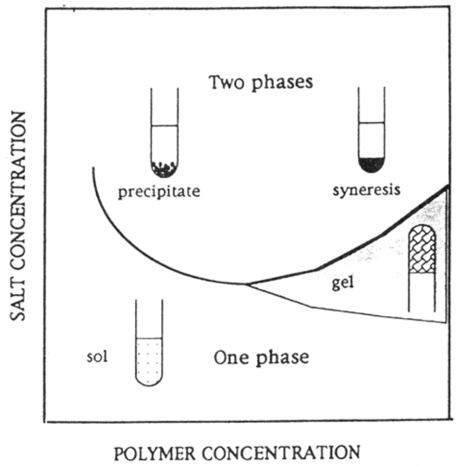

Figure 1. Synoptic representation of the phase diagrams: (—) the demixing line which separates the "one phase" and "two phase" domains; (- - -) sol–gel transition line.

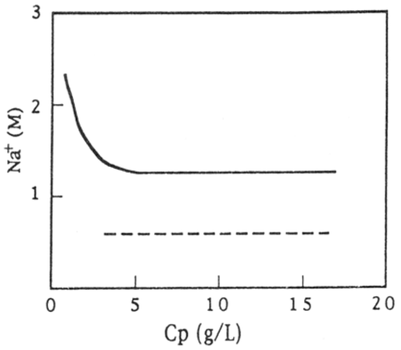

Figure 2. H type diagrams: demixing lines for alginates (ξ = 1.6) + NaCl, pH 4 (—), and for a high methoxyl pectin (ξ = 0.44) + NaCl, pH 7 (- - -).

ent phase is observed which could be either a solution or a gel. Above this line, two phases appear: a transparent poor polymer phase in equilibrium with a rich polymer phase which could be a precipitate, large aggregates of microgels, or a dense uniform gel.

The classification of the different types of phase diagrams can be derived from the Ikegami and Imai models,[20] by considering first the characteristics of the demixing lines. The changes in the shape and the shift of the demixing line ($[\mathrm{M}^{n+}]^* = f(C_p)$) as a function of ξ are taken as the basis for a more detailed classification. The H type implies that $[\mathrm{M}^{n+}]^*$ required at the phase separation is high, is independent of C_p, and is an increasing function of ξ (Figure 2). The L type corresponds to an increasing linear variation of $[\mathrm{M}^{n+}]^*$ with C_p, the slope of which increases with ξ, and to very small values of $[\mathrm{M}^{n+}]^*$.[20,33,34] However, Figures 3 and 4 are examples of systems that correspond to neither the H nor L type: the higher the value of ξ, the lower the value of $[\mathrm{M}^{n+}]^*$, and the demixing curves are concave. This behavior, called the I type, is an intermediate one which lies between weak ion–polyion interactions corresponding to the H type and stronger interactions corresponding to the L type.

Subdivisions in this first classification may be introduced by considering the existence of a gel phase. To summarize, the following diagrams may be identified:

–sol diagrams where only a solution phase is observed in the whole C_p and $[\mathrm{M}^{n+}]$ ranges investigated.

–H type, I type, and L type diagrams where precipitates or large aggregates without any cohesion are formed from the solutions above the demixing lines.

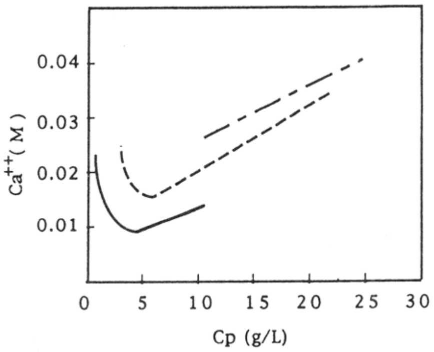

Figure 3. I type diagrams: demixing lines for PAM + CaCl_2 (pH 7 in pure water): ξ = 0.49 (— — —), ξ = 0.78 (- - -), ξ = 1.15 (—).

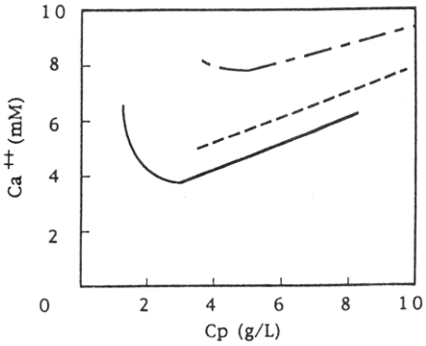

Figure 4. I type diagrams: demixing lines for PEC + CaCl_2 (NaCl 0.1 M and pH 7): ξ = 0.84 (— — —), ξ = 0.90 (- - -), ξ = 1.16 (—).

–(I type + gel/S) diagrams where precipitates or compact gels with syneresis are formed, above the demixing lines of the I type, depending on the polymer concentration.

–(type I + gel) and (type L + gel) diagrams where below the demixing line of the I and L types, respectively, solutions at low C_p and homogeneous gels (without syneresis) at higher C_p are observed. In these cases, above the demixing line, precipitates and gels with syneresis are obtained from the solutions and the gels, respectively.

As discussed later, the occurrence of such diagrams depends on the ion–polyion interactions as well as on some properties of the polymer (flexibility, charge distribution, hydrophobicity of the nonionic part).

A. Phase Diagrams in Pure Water. Table 1 shows the types of diagrams obtained in the absence of NaCl reported as a function of ξ. In all the tables and figures, ξ is given for α = 1, whatever the pH.

A first general remark can be made: the salting out of solutions of the two natural polymers investigated is much easier than that of PAM, for the same charge density. A precipitation of H type is observed with pectins at pH 7 and alginates at pH 4 in the presence of NaCl while PAM remains soluble, regardless of the pH between 4 and 7, until the saturation concentration of NaCl in water is reached. The precipitation cannot be attributed to the formation of ion–polyion complexes. Flory's approach[28] considers two terms in the second virial coefficient, one corresponding to the nonelectrostatic and a second one to electrostatic interactions. The latter term tends to zero when the ionic strength increases and precipitation can only take place if the nonionic second virial coefficient is negative. The low stability of the pectins and alginates reflects a negative contribution to the virial coefficient of the nonionic part of the molecules. Figure 2 shows that precipitation of high-methoxyl pectin occurs at a lower NaCl concentration than precipitation of alginate. This

Table 1. Types of Diagrams Observed for the Different Series of Polymers as a Function of the Charge Parameter, Calculated for Fully Ionized Carboxylate Groups

Acrylamide–Acrylic Acid Copolymers, AD Series

	ξ				
	0.043	0.20	0.49	0.78	1.01
Na	sol	sol	sol	sol	sol
Mg	sol	sol	sol		type H
Mn	sol	sol	sol	sol	type I
Ca	sol	sol	type I	type I	type I
Cu	sol	type I + gel/S	type I + gel/S	type I + gel/S	

Acrylamide–Acrylic Acid Copolymers, H Series

	ξ				
	0.043	0.57	0.86	1.15	1.44
Ca	sol	sol	type I	type I + gel/S	type I + gel/S

Pectinates (PEC) and Alginates (ALG)

	PEC $\xi = 0.44$	PEC $\xi = 0.9$	PEC $\xi = 1.16$	ALG $\xi = 1.6$
Na	type H	type H	type H	type H
Ca	type H	type I + gel	type I + gel	
Cu	type L + gel	type L + gel	type L + gel	type I + gel

is due to the higher hydrophobicity of the pectin caused by the presence of methyl groups on its backbone. Another example for the Flory principle is PAM where the presence of amide groups hinders precipitation.

When multivalent ions are concerned, a similar shift of behavior of lower stability and higher interactions are observed between the synthetic and natural polymers. For example, the $[M^{n+}]^*$ values obtained in the presence of Ca^{2+} are significantly lower for pectins than for PAM, for the same charge density, as shown by the comparison of Figures 3 and 4.

An important observation is the reactivity series obtained for all polymers:

$$Mg^{2+} < Mn^{2+} < Ca^{2+} < Cu^{2+}$$

In the case of the PAM series, the four divalent cations exhibit demixing lines of the I type and no true gelation without syneresis occurs. Besides, this reactivity series is reflected by the decrease in the value of ξ above which phase separation occurs as the strength of the interaction increases (Table 1).

If these results show the role played by the nature of the cation and the charge parameter of the polymer, the difference in the behaviors of the AD and H series of PAM is clearly governed by the charge distribution along the chain (Table 1). Indeed, in the case of AD where the charge distribution is quasi Bernouillan, the addition of Ca^{2+} induces precipitation of the polymer in the form of a white and dense powder. Under the same conditions, gels are formed (I type + gel/S) in the region of the phase separation for H series where many more isolated COO^- groups are present along the chain. The presence of carboxylate sequences in the AD series allows intramolecular cation binding which leads preferentially to precipitation, whereas the absence of such sequences in the H series favors cross-linking and formation of an infinite network.

In the case of pectins and alginates, despite less information, the same general trends can be observed. Indeed, Table 1 shows that, when the influence of Ca^{2+} on the PEC series is considered, there is a threshold in ξ values above which gelation occurs, while below this threshold only phase separation of the H type is observed. Nevertheless, even if the affinity order is the same for both synthetic and natural polymers, the strength of the interactions for a given cation is polymer dependent. Thus, the Ca^{2+} effect on the PEC series seems to be comparable to that of Cr^{n+} on the PAM series, and in a similar way, Cu^{2+}/PEC and Al^{n+}/PAM systems exhibit the same behaviors.[59] Hence, by analogy with phase diagrams of PAM, one may predict I type or L type precipitation, with Ca^{2+} and Cu^{2+}, respectively, for higher values of ξ. The presence of a gel phase, which seems to be a more frequent feature in these natural polymers, must be related to the predominance of interchain associations. These junction zones result in the dimerization of polygalacturonic or polyguluronic sequences in a regular conformation with interchain chelation of extented arrays of cations on specific binding sites along the chain. This structure is known as the "egg box" model.[60]

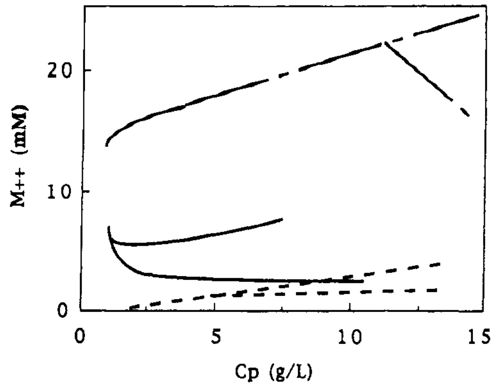

Figure 5. Phase diagrams for a pectin sample with $\xi = 1.16$ at pH 7 in NaCl 0.1 M + $CuCl_2$ (- - -), + $CaCl_2$ (—), and + $MnCl_2$ (— – —).

Table 2. Variation of $[Ca^{2+}]^*$ and $[Cu^{2+}]^*$ as a Function of the Concentration of NaCl, for PAM and PEC Series

		[NaCl], M			
		0	0.05	0.1	1
$[Ca^{2+}]^*$, M	AD ($\xi = 1.15$)	0.01			0.10
	H ($\xi = 1.15$)	0.03			0.15
	H ($\xi = 1.07$)	0.01	0.03	0.10	∞
$[Cu^{2+}]^*$, M	AD ($\xi = 0.20$)	0.004		0.007	
	AD ($\xi = 0.49$)	0.002		0.004	
	AD ($\xi = 0.78$)	0.001		0.0035	
$[Cu^{2+}]^*$, M	PEC ($\xi = 0.44$)	1.3×10^{-3}		4×10^{-4}	
	PEC ($\xi = 1.16$)	2×10^{-3}		7.2×10^{-4}	
$[Ca^{2+}]^*$, M	PEC ($\xi = 1.16$)	5.4×10^{-3}		4×10^{-3}	

It is also interesting to consider in greater detail the features of the sol–gel transition line. Indeed, it must be noted that the sol–gel transition line always displays a positive slope in the phase separation of the L type (Figure 5) and that a large drop of this line is observed at low C_p followed either by a slightly negative slope or by a constant value when C_p increases in the case of a phase separation of the I type, as illustrated in Figure 5.

B. Phase Diagrams in the Presence of NaCl. The phase diagrams of the same systems were also established in the presence of NaCl. Table 2 illustrates the influence of NaCl on the $[Ca^{2+}]^*$ and $[Cu^{2+}]^*$ values, in the case of the PAM and PEC series.

The increase of $[Ca^{2+}]^*$ when [NaCl] increases means that this monovalent salt reduces the destabilizing power of Ca^{2+}. At a low enough $[Ca^{2+}]^*$, in the absence of NaCl a polymer precipitate can be formed which may then dissolve on addition of NaCl. This behavior may be simply interpreted in terms of a competition between Na^+ and Ca^{2+} if their interactions with the polyions are determined by equilibrium laws. Even if the binding constant of Na^+ is expected to be much lower than that of Ca^{2+}, a large excess of Na^+ with respect to Ca^{2+} will be able to remove

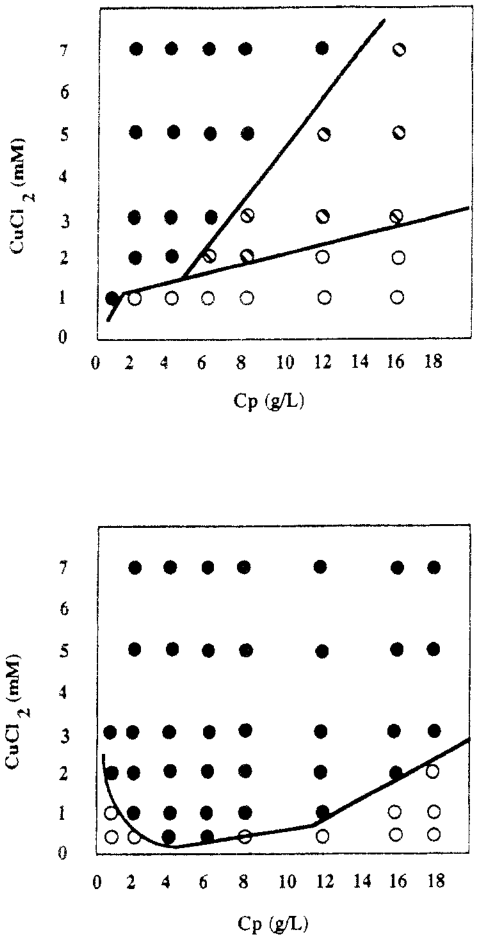

Figure 6. Influence of NaCl for the alginate + $CuCl_2$ at pH 4.8. The phase diagram on the top corresponds to NaCl = 0 M, while the one on the bottom corresponds to NaCl 0.5 M. Key: (—) the demixing line; (- - -) the sol–gel transition line; (○) sol; (●) precipitate; (⊖) gel.

Ca^{2+} from the polyion. Since PAM is completely soluble in NaCl solutions up to its saturation concentration, the polymer recovers its solubility. It is quite clear that in such a scheme the relative excess of Na^+ required to obtain the solubilization will depend on the charge parameter of the polymer if the same ratio $[M^{2+}]/[COO^-]$ is considered. For example, a precipitate of PAA formed at pH 7 by addition of Ca^{2+} or Ba^{2+} cannot be redissolved by NaCl. This salt effect is a common feature of PAM. It was also observed with Cu^{2+} and Ba^{2+}.

For alginate samples in the presence of Cu^{2+}, it was observed that an increase of NaCl concentration leads to a general lowering of the demixing line concomitantly with a decrease of the slope (Figure 6). As indicated in Table 2, a similar effect on addition of sodium salts was also found in the pectin samples at a range of ξ values between 0.44 and 1.16 with either the L or I type of phase diagram. Thus the zone of the phase separation expands as the salt concentration increases. A possible explanation is that the addition of NaCl in the presence of a divalent cation in such systems acts so as to decrease the second virial coefficient of the macromolecule by screening the remaining charges. This allows the hydrophobic interactions to take place in the case of pectins or the hydrogen bonds in the case of alginates. Resolubilization by an excess of NaCl cannot be expected for these polymers.

C. Influence of the pH on the Phase Diagrams. The variation of ξ for a given polymer series must be obtained either by changing τ (Figures 3 and 4 for PAM and PEC, respectively, with $CaCl_2$) or by changing the pH for a given τ. For PAM samples with Ca^{2+} it was reported[31,32] that a decrease of pH from 7 to 3 decreased the charge density and moved the demixing line upward, as expected to I type behavior. In this case the presence of $CONH_2$ or COOH groups instead of COO^- is equivalent in terms of polymer solubility. PEC samples with Ca^{2+} also exhibit an I type behavior at $\alpha = 1$ for different τ. Here it was found that a decrease of pH in the same range led to a slightly lower demixing line.[38] This phenomenon may be explained by the strengthening of intramolecular hydrophobic interactions between the CH_3 groups as the number of charged groups declined. Finally, the behavior of the alginate sample with changing pH in the presence of Mn^{2+} was similar to that of PAM as expected for a polymer with a hydrophilic nonionic part (results not shown). At very low pH all these polymers are nonsoluble.

Discussion

In the previous section, we have tried to draw some general conclusions from the comparison between the different systems investigated. We propose here a more theoretical approach which may be the basis of a quantitative comparison of the demixing and sol–gel transition lines.

A. Demixing Lines of the H, I, and L Type. We will consider the simple model previously proposed by Strauss[17] to explain the phase separation phenomena. The polyelectrolyte, in interaction with divalent cations, was considered as a copolymer and composed of ionized monomer units A and adjacent monomer units B neutralized by the divalent cation, according to the following model:

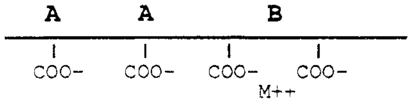

Since the B units are insoluble, the solubility of the polymer is due to the presence of A units. Demixing can only be expected above a given number of B units along the chain. Such a model would lead to a linear variation of $[M^{2+}]^*$ versus C_p and is unable to explain our intermediate I type demixing. Moreover, the role played by the neutral monomer units (B) present in our samples and their contribution to the excluded volume effect is not taken into account.

Let us consider a solution of a polyelectrolyte constituted of A units, B units, and other neutral units C: the molar ratio C/[A + 2B + C] is defined by the chemistry while the ratio f = 2B/[2B + A] depends on the ion–polyion interactions.

The free energy (F) of such a solution may be written, according to Flory,[28] as a sum of three terms.

(a) A nonelectrostatic term, due to the C neutral units:

$$\frac{F_C}{kT} \cong \frac{1}{2}\upsilon_c(1-\tau)^2{C_p}^2 + \frac{1}{3}{w_c}^2(1-\tau)^3{C_p}^3 \tag{3}$$

where υ_c is the excluded volume parameter and w_c is the third virial coefficient. Under the relatively high dilution conditions used in this work the term in ${C_p}^3$ can be neglected and eq 3 is reduced to the excluded volume term.

(b) A coulombic term corresponding to the electrostatic repulsion between the charges of A units:

$$\frac{F_A}{kT} \cong \frac{1}{2N_A I}\tau^2(1-f)^2{C_p}^2 \tag{4}$$

where N_A is the Avogadro number. No excluded volume parameter for the A units has been introduced in eq 4 because of the preponderant effect of the electrostatic contribution.

(c) A third term corresponding to the B units:

$$\frac{F_B}{kT} \cong \frac{1}{2} \upsilon_B \frac{\tau^2 f^2}{4} C_p^{\,2} \tag{5}$$

where υ_B is the associated excluded volume parameter which is assumed to be negative.

The total free energy is then

$$\frac{F}{kT} = \frac{F_A}{kT} + \frac{F_B}{kT} + \frac{F_C}{kT} \tag{6}$$

and the demixing occurs when

$$\frac{\delta^2 F}{\delta C_p^{\,2}} = 0$$

This means

$$\upsilon_c(1-\tau)^2 + \frac{\tau^2(1-f)^2}{N_A I} + \frac{\upsilon_B \tau^2 f^2}{4} = 0 \tag{7}$$

Let us now analyze the situation under two distinct conditions.

(a) In the absence of multivalent cations. Relation 7 is reduced to

$$\upsilon_c(1-\tau)^2 + \frac{\tau^2}{N_A I} = 0 \tag{8}$$

This condition is respected for a given critical ionic strength I^*:

$$I^* = -\frac{\tau^2}{\upsilon_c(1-\tau)^2 N_A} \tag{9}$$

(i) If $\upsilon_c > 0$, that is to say when the excluded volume parameter of the neutral units is positive, no phase separation is expected as I increases. This is likely to occur in PAM and is consistent with data on the thermodynamic behavior of the homopolyacrylamide which exhibits a positive second virial coefficient in pure water and in the presence of NaCl.[61]

(ii) If $\upsilon_c < 0$, at a critical ionic strength given by (9), a phase separation must occur. Alginates and pectins in excess of NaCl illustrate such a behavior.

Expression 9 shows that I^* does not vary with C_p. This prediction is in rather good agreement with the shape of the demixing curves of the H type represented in Figure 2.

(b) In the presence of multivalent cations. (i) In pure water, the three terms of eq 7 must be taken into account. If we introduce the ionic strength due to the free charges of the polyions as $I = C_p \alpha \tau (1-f)$, then eq 7 becomes

$$\upsilon_c(1-\tau)^2 + \frac{\tau(1-f)}{\alpha N_A C_p} + \upsilon_B\left(\frac{\tau f}{2}\right)^2 = 0 \tag{10}$$

The demixing will require a critical fraction, f^*, which will depend on υ_c, C_p, and τ.

(ii) In a large excess of NaCl, I = [NaCl] and the second term of eq 10 vanishes. Then two situations must be considered.

In the first situation, the excess of NaCl is enough to completely remove the multivalent cations, causing the B units to disappear and the third term of eq 10 to vanish. The solubility depends on the υ_c value alone. If $\upsilon_c > 0$, a solution is expected; this explains well why a precipitate of a slightly charged PAM can be dissolved by an excess of NaCl. If $\upsilon_c < 0$, no solubilization is expected.

The second situation occurs when not all the multivalent cations are removed by NaCl. The third term of (10) remains and a phase separation will occur for a value of f which again depends on υ_c and τ but is independent of C_p.

We can now try to predict on the basis of these considerations, at least qualitatively, the shape of the demixing curves. The problem involves calculating the amount of multivalent cations added at the demixing $[M^{2+}]^*$ as a function of C_p.

Let us use a simple model where, in pure water, the formation of B species is assumed to be governed by the following equilibrium:

$$2[COO^-] + [M^{2+}]_f \overset{K_B}{\rightleftarrows} [(COO)_2M]$$

At the onset of phase separation, the critical $[M^{2+}]^*$ is given by

$$[M^{2+}]^* = [(COO)_2M]^* + [M^{2+}]_f^* \tag{11}$$

where $[(COO)_2M]^*$ and $[M^{2+}]_f^*$ are respectively the complex and the free M^{2+} concentrations at the demixing. By definition:

$$[COO^-]^* = (1-f)^* \tau C_{pM} \tag{12}$$

$$[(COO)_2M]^* = f^* \tau C_{pM}/2 \tag{13}$$

where C_{pM} is the total molar concentration of monomers. By introducing, in the relation 11, the values of $[COO_2M]^*$ given by (13) and $[M^{2+}]_f^*$ given by (12) and (13) and the following equilibrium

$$[(COO)_2M]^* = K_B[M^{2+}]_f^*[COO^-]^{*2} \tag{14}$$

one arrives at

$$[M^{2+}]^* = \frac{f^* \tau C_{pM}}{2} + \frac{f^*}{2K_B \tau C_{pM}(1-f^*)^2} \tag{15}$$

If f^* can be considered as independent of C_p and τ, this last equation (15) may describe the I and L types of the demixing curves. If K_B is very high, as in the case of very strong interactions, the second term of (15) can be neglected and a linear variation of $[M^{2+}]^*$ versus C_p expected (L type). Indeed, such behavior has been obtained with some systems such as PEC/Cu^{2+}. In that case, the correlation between this type of line L and a high value of K_B is well verified. In addition, potentiometric measurements show that all ions added to the solutions are completely bound to the polymer, with a stoichiometry of 2, when polymer saturation is reached.[62] Moreover, in that case, the slope of $[M^{2+}]^* = f(C_p)$ must be proportional to τ, as has been observed.

For lower values of K_B and τ, the second term of (15) is predominant at low C_p, and thus $[M^{2+}]^*$ is shown to decrease with C_p. Conversely, the first term dominates at higher C_p; therefore a minimum in $[M^{2+}]^*$ must be observed and the asymptotic curve is a straight line. This is exactly what was observed in the I type. PAM/Ca^{2+}

and PEC/Ca^{2+} systems are good examples of such a behavior, and it has been shown that the polymers considered here are able to bind only a fraction of the cations, which decreases with ξ.[32,63] Below the value of C_p where the asymptote is reached, and when the second term of (15) is predominant, $[M^{2+}]^*$ is expected to decrease when τ increases. This is well consistent with the results shown in Figures 3 and 4.

Finally, the changes in the demixing lines as [NaCl] increases must be discussed. From relation 7 a lower fraction f^* should be necessary as NaCl increases since the electrostatic term decreases with I. If the values of $[M^{2+}]^*$ at which f^* is reached does not depend on [NaCl], a decrease of $[M^{2+}]^*$ with [NaCl] is also expected. Such a dependence was well observed in the PEC/Cu^{2+} system but not in the case of PAM, whatever the nature of M^{n+} (Table 2). In fact, if we consider a competition between Na^+ and M^{n+} and introduce a second equilibrium

$$[COO^-] + [Na^+]_f \overset{K_{BNa}}{\rightleftarrows} [COONa]$$

we can understand that even if the f^* value is lower, the value of $[M^{2+}]^*$ for which $f = f^*$ may be higher than in the absence of NaCl. The behavior of PAM/M^{n+} can be reconciled with our model in this way. It is obvious that the shift of $[M^{2+}]^*$ toward higher values will depend on the ratio $K_{BNA}{}^2/K_B$. The shift can be large and resolubilization can occur if the constant K_B is low (e.g. PAM/Ca^{2+}); only a slight increase of $[M^{2+}]^*$ is expected for a very strong polymer/M^{n+} interaction. The decrease of $[M^{2+}]^*$ in the case of PEC/Cu^{2+} is also compatible with this analysis: the ratio $K_{BNA}{}^2/K_B$ is very low with phase separation following the addition of NaCl. For PEC/Ca^{2+} the slight decrease of $[Ca^{2+}]^*$ with NaCl may result in an increase of $[Ca^{2+}]^*$ due to the competition Na/Ca and a decrease of $[Ca^{2+}]^*$ due to the phase separation facilitated by the NaCl.

Though the model proposed here allows a qualitative explanation of experimental data, many aspects of the problem are still not taken into account. What remains to be determined is the type of behavior for which it may be quantitatively applicable.

(i) In the equilibrium equation we introduce the total concentration of carboxylate groups as if they were small isolated ions. This means that we disregard (1) the polyelectrolyte effect which tends to concentrate the counterions in the immediate vicinity of the polyion and increases when ξ increases and (2) the possible effect of the charge distribution along the chain. The first effect tends to vanish when C_p increases and may be reasonably neglected when $C_p > C_p^*$, the critical overlap concentration of the chain. Such an approximation is acceptable in certain situations. For example it has been shown that the amount of Cu ions bound on the PEC depends only on the total concentration of ionized carboxylate groups whatever the value of ξ. The same value of K_B allowed the adjustment of the experimental and calculated values of the fraction of bound Cu ions.[62] However, in the case of Ca^{2+} and Cu^{2+} which interact less strongly with PAM, the binding constant has been found to decrease when ξ decreases.[64,65] Moreover, as discussed above, the binding and the relative proportion of intra- and intermolecular complexes are related to the distribution of the charges, as in the case of Ca^{2+}. This effect disappears at higher charge density and for stronger interactions. Our model may be useful when the interactions are very strong and the polymer concentration high; it probably fails when interactions are weaker and the polymer concentration is low. Correction of the concentration of the ionic species, to take into account the counterion accumulation (through, for example, the Weisbuch and Gueron approach) may constitute a possible improvement to our model. The development of a model of discrete charges may also help to resolve the problem of charge distribution along the chain.

(ii) No distinction is made in the third term of the free energy between the contributions of the inter- and intramolecular complexes. This may not be important for synthetic polymers, of the concentration range investigated in this work, since intermolecular complexes can be neglected with respect to the intra. In the case of natural polymers that give phase diagrams of type I (L) + gel, the intermolecular bindings become preponderant over a given concentration due to the intrinsic rigidity of the polymeric chain[47] and should therefore take into account the quantification of $[M_2{}^+]^*$.

(iii) In a similar manner, if we consider a unique type of neutral units while decreasing the pH, the number of un-ionized carboxylate groups (COOH) must increase. This must contribute to a change in the value of f^* according to the excluded volume parameter attributed to such species.

(iv) Only biliganded complexes are considered. For divalent cations, we neglect a possible step of monoligandation, and for ions of higher charge, the stoichiometry of the complex may be higher. This does not significantly change our conclusion in general. However, when the charge of the cations is known to change gradually with the concentration as in the case of chromium, the shape of the demixing curve must also alter.

B. Sol–Gel Transitions. The formation of an infinite network from a semidilute solution of polymer requires the formation of at least one cross-link per macromolecular chain.[66] In order to understand the sol–gel transition lines we must introduce the concept of intermolecular binding which is neglected as far as phase separation alone is considered. The variation of the critical concentration of the free complexing ions at the sol–gel transition $[M^{2+}]f_{gel}$ has been calculated by Pezron and Leibler,[67] for a nonionic polymer: $[M^{2+}]f_{gel}$ is predicted to vary as $C_p{}^{-1/(3\nu-1)}$ if ν is the excluded volume exponent of the polymer–solvent system. Under good solvent conditions, a decrease of $[M^{2+}]f_{gel}$ as a function of $C_p{}^{-1.25}$ is predicted. This exponent has been verified in the case of the galactomannan/borax system.[67] The results indicate that the same exponent was found for the system PEC/Ca with $\xi = 0.9$ and in 0.1 M NaCl. However, in the presence of added NaCl for larger ξ values or in pure water the value of the exponent was found to be lower. Obviously, the polyelectrolytic character of our systems introduces a higher degree of complexity. Nevertheless, we will use a reasoning similar to Pezron and Leibler's, by also taking into account the specific behavior of the polyelectrolytes.

In the isotropic model of the semidilute solutions of polyelectrolytes,[68,69] the concentration [E] of polymer–polymer contacts and/or entanglements varies as $1/\xi_s{}^3$, if ξ_s is the screening length associated with the temporary network defined by Edwards.[70] According to Pfeuty,[71] ξ_s varies as $C_p{}^{-1/2}(\alpha\tau)^{-1/3}$ and $C_p{}^{-3/4}(\alpha\tau)^{-1/2}\kappa^{1/2}$ (κ is the Debye length) in the absence and in the presence of salt, respectively. These predictions have been verified in the case of PAM.[36]

If the formation of the cross-links is assumed to be governed by an equilibrium of the type

$$[E] + [M^{2+}]_f \overset{K_{BInter}}{\rightleftarrows} [EM]$$

the concentration of cross-links [EM] is

$$[\mathrm{EM}] = K_{\mathrm{BInter}}[\mathrm{E}][\mathrm{M}^{2+}]_{\mathrm{f}} \tag{16}$$

Since the condition of gelation can be written [EM] = C_{pM}/N, that is the molar concentration of chain, where N is the degree of polymerization, and by assuming that this limit is much lower than the total number of polymer–polymer contacts in the solution, one obtains the following value for the concentration of free M^{2+} at the transition, $[M^{2+}]f_{\mathrm{gel}}$, in the absence of salts:

$$[\mathrm{M}^{2+}]_{\mathrm{fgel}} \approx N^{-1}K_{\mathrm{BInter}}^{\ -1}C_{\mathrm{p}}^{\ -0.5}(\alpha\tau)^{-1} \tag{17}$$

and in the presence of salts

$$[\mathrm{M}^{2+}]_{\mathrm{fgel}} \approx N^{-1}K_{\mathrm{BInter}}^{\ -1}C_{\mathrm{p}}^{\ -1.25}(\alpha\tau)^{-1.5}\kappa^{1.5} \tag{18}$$

To calculate the salt concentration $[M^{2+}]_{\mathrm{gel}}$ at the transition, the equilibrium of intramolecular binding must also be taken into account, through relations 11 and 14, and applied to the sol–gel transition

$$[\mathrm{M}^{2+}]_{\mathrm{gel}} = N^{-1}K_{\mathrm{BInter}}^{\ -1}C_{\mathrm{p}}^{\ -0.5}(\alpha\tau)^{-1}[1 + K_{\mathrm{B}}(\alpha\tau C_{\mathrm{p}})^2] \tag{19}$$

and

$$[\mathrm{M}^{2+}]_{\mathrm{gel}} = N^{-1}K_{\mathrm{BInter}}^{\ -1}C_{\mathrm{p}}^{\ -1.25}(\alpha\tau)^{-1.5}\kappa^{1.5}[1 + K_{\mathrm{B}}(\alpha\tau C_{\mathrm{p}})^2] \tag{20}$$

in the absence and in the presence of salt, respectively. In these expressions, $[COO^-]_{\mathrm{gel}}$ is approximated at $\alpha\tau C_p$ because the sol–gel transition occurs at low values of $[M^{2+}]$ and the concentration $[(COO)_2M]_{\mathrm{gel}}$ must be small.

These expressions predict a decrease of $[M^{2+}]_{\mathrm{gel}}$ when $\alpha\tau$ increases. This has been verified in the case of the PEC/Ca^{2+} system in the presence of NaCl[39] for which the sol–gel transition lines are significantly shifted toward lower values of $[M^{2+}]$ when the charge parameter increases. Figure 7 shows that by plotting $[M^{2+}]_{\mathrm{fgel}}(\alpha\tau)^{1.5}$ as a function of C_p, the lines can be almost superimposed, as predicted by relation 18, with any remaining differences coming from the term in K_B. Indeed, in the case of pectins the probability of the formation of a junction zone [EM], for a given charge distribution, depends on τ since a minimum number of carboxylate groups are required for its formation. Thus we have observed, as expected from (18), an increase of $[M^{2+}]_{\mathrm{fgel}}$ as K_B, and therefore τ decreases.

If the term $[1 + K_B(\alpha\tau C_p)^2]$ in relations 19 and 20 can be approximated to 1, that is to say in the case of weak ion–polyion interactions, we arrive again at the predictions of Pezron and Leibler[67] for the C_p dependence of $[M^{2+}]_{\mathrm{gel}}$, at least when NaCl is present. The absolute value of the exponent is much lower in the absence of salt. In both cases, a decrease of $[M^{2+}]_{\mathrm{gel}}$ with C_p is expected, as was observed for PEC/Ca and PEC/Mn (Figures 5 and 7). If, on the contrary, the interactions are too strong to allow this term, $[1 + K_B(\alpha\tau C_p)^2]$, to be neglected, the slope of the variation of $[M^{2+}]_{\mathrm{gel}}$ versus C_p may be close to 0 and may even become positive. This was observed in various systems such as PEC/Cu (positive slope). Greater knowledge of $[M^{2+}]_{\mathrm{fgel}}$ as opposed to $[M^{2+}]_{\mathrm{gel}}$ could improve our comprehension of these systems.

Conclusion

The comparison of phase diagrams obtained with natural and synthetic polyanions led to the following conclusions. The behavior of several systems, that at first seem to be quite different from each other, can be described by a single general scheme in which the free energy of the solutions is expressed as the sum of several contributions and which considers binding equilibria of the multivalent cations on the polyions. Electrostatic interactions have not necessarily the preponderant role; within the low charge density and the high ionic strength limits, the nonionic interactions, due to the presence of hydrophobic units, must also be taken into account. This hydrophobic effect explains partially some differences observed in the phase diagrams of synthetic and natural polymers.

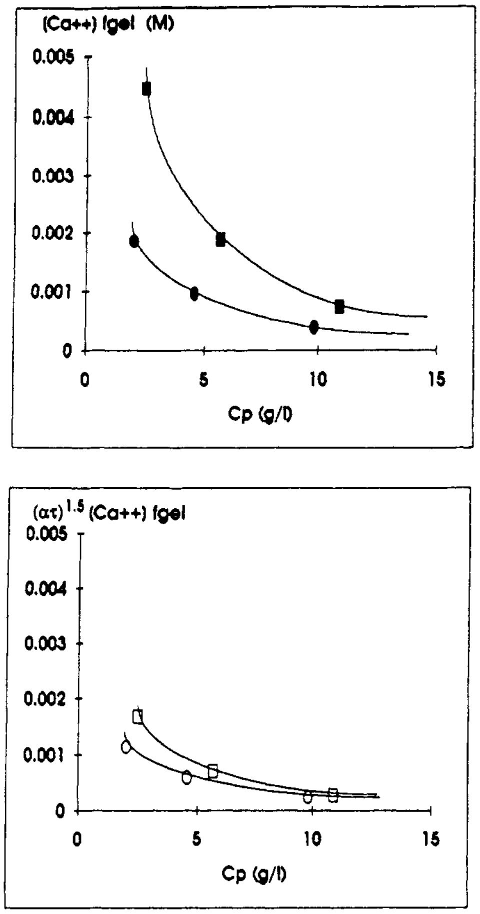

Figure 7. Evolution of the free calcium concentration at the sol–gel transition for pectin samples with $\xi = 0.84$ (■) and with $\xi = 1.16$ (●). The empty symbols in the bottom graph show the reduced free calcium concentration following eq 20.

Our analysis could serve as a basis for a quantitative prediction of the demixing and sol–gel transition. To this end a knowledge of the binding constants which are considered in the equations would be necessary. Measuring the binding isotherms of the cations will be required to ascertain our approach and eventually to improve the proposed scheme.

In addition we can also conclude from the comparison of phase diagrams that biological polymers possess a much higher affinity for multivalent cations than synthetic ones even if the order of affinity toward different cations is the same for both types of polymers. This is probably due to differences in the details of the microstructure and in the flexibility of the backbone. The formation of junction zones implies at least two chains, giving greater rigidity and leading to a particular stereochemistry in the case of PEC and alginate in relation to their biological role. Determination of the structure of the intra- and intermolecular complexes and of the number of chains implied in the junction zones, through rheological and scattering measurements, will contribute to further understanding of the different patterns of behavior observed for the various polymers.

Acknowledgment. The authors thank Mr. K. El Brahmi, L. Want, C. Garnier, S. Meuleumans, M. D. Petit, S. Twitchen, and C. Ouwerx for the determination of the phase diagrams as well as M. Rawiso, J. F. Thibault, and N. Velings for fruitful discussions.

References and Notes

(1) Manning, G. S. *J. Chem. Phys.* **1969**, *51*, 924.
(2) Manning, G. S. *Q. Rev. Biophys.* **1978**, *11*, 179.
(3) Iwasa, K.; Kwak, J. C. T. *J. Phys. Chem.* **1977**, *81*, 408.
(4) Joshi, Y. M.; Kwak, J. C. T. *J. Phys. Chem.* **1979**, *83*, 1978.
(5) Mattai, J.; Kwak, J. C. T. *Macromolecules* **1986**, *19*, 1663.
(6) Racape, E.; Thibault, J. F.; Reitsma, J. C. E.; Pilnik, W. *Biopolymers* **1989**, *28*, 1435.
(7) Rinaudo, M.; Milas, M. *J. Polym. Sci.* **1974**, *12*, 2073.
(8) Rinaudo, M. In *Polyelectrolytes*; Sélégny, E., Ed.; D. Reidel Publishing Co.: Dordrecht, Holland, 1974; p 157.
(9) Kohn, R. *Pure Appl. Chem.* **1975**, *42*, 371.
(10) Koblansky, M.; Zema, P. *Macromolecules* **1981**, *14*, 1448.
(11) Meurer, B.; Spegt, P.; Weill, G. *Biophys. Chem.* **1982**, *16*, 89.
(12) Debongnie, P. Ph.D., Louvain-la-Neuve, 1991.
(13) Koblansky, M.; Zema, P. *Macromolecules* **1981**, *14*, 166.
(14) Cantor, C. R.; Schimmel, P. R. *Biophysical Chemistry, Part III: The Behaviour of Biological Macromolecules*; W. H. Freeman and Co.: San Francisco, 1980; p 849.
(15) Gueron, M.; Weisbuch, G. *J. Phys. Chem.* **1979**, *83*, 1991.
(16) Gueron, M.; Weisbuch, G. *Biopolymers* **1980**, *19*, 353.
(17) Armstrong, R. W.; Strauss, U. P. In *Encyclopedia of Polymer Science and Technology*; Mark, H. F., Gaylord, N. G., Bikales, N. M., Eds.; Wiley-Intersciences: New York, 1969; Vol. 10, p 781.
(18) Strauss, U. P.; Ander, P. *J. Am. Chem. Soc.* **1958**, *80*, 6494.
(19) Eisenberg, H.; Woodside, D. *J. Chem. Phys.* **1962**, *36*, 1844.
(20) Ikegami, A.; Imai, N. *J. Polym. Sci.* **1962**, *56*, 133.
(21) Buscall, R.; Corner, T. *Eur. Polym. J.* **1982**, *18*, 967.
(22) Michaeli, I. *J. Polym. Sci.* **1960**, *48*, 291.
(23) Strauss, U. P.; Siegel, A. J. *J. Phys. Chem.* **1963**, *67*, 2683.
(24) Strauss, U. P.; Leung, Y. P. *J. Am. Chem. Soc.* **1965**, *87*, 1476.
(25) Napper, D. H. *J. Colloid. Interface Sci.* **1970**, *33*, 385.
(26) Dubin, P. L. In *Structure-solubility relationships in Polymers*; Academic Press: New York, 1977.
(27) Eisenberg, H.; Mohan, G. R. *J. Phys. Chem.* **1959**, *63*, 671.
(28) Flory, P. J. *J. Chem. Phys.* **1953**, *21*, 162.
(29) Schwartz, T.; François, J. *Makromol. Chem.* **1981**, *182*, 2775.
(30) Truong, N. D.; Galin, J. C.; François, J.; Pham, Q. T. *Polym. Commun.* **1984**, *25*, 208.
(31) Truong, N. D. Ph.D., Strasbourg, 1984.
(32) Truong, N. D.; François, J. In *Solid-liquid interactions in porous media*; Technip: Paris, 1985; No. 42, p 251.
(33) Rabhari, R.; François, J. *Polymer* **1988**, *29*, 851.
(34) Rabhari, R.; François, J. *Polymer* **1992**, *33*, 1449.
(35) El Brahmi, K.; Rawiso, M.; François, J.; Mestdagh, M. M. *Polym. Commun.*, submitted for publication.
(36) El Brahmi, K. Ph.D., Strasbourg, 1991.
(37) Allain, C.; Salomé, L. *Macromolecules* **1990**, *23*, 981.
(38) Garnier, C.; Axelos, M. A. V.; Thibault, J. F. *Carbohydr. Res.* **1993**, *240*, 219.
(39) Garnier, C. Ph.D., Nantes, 1992.
(40) Kulkarni, R. A.; Gundiah, S. *Makromol. Chem.* **1984**, *185*, 969.
(41) Reed, W. F.; Ghosh, S.; Medjahdi, G.; François, J. *Macromolecules* **1991**, *24*, 6189.
(42) Truong, N. D.; Medjahdi, G.; Sarazin, D.; François, J. *Polymer. Bull.* **1990**, *24*, 101.
(43) El Brahmi, K.; Rawiso, M.; François, J. *Eur. Polym. J.* **1993**, *29*, 1531.
(44) Truong, N. D.; Galin, J. C.; François, J.; Pham, Q. T. *Polymer* **1986**, *27*, 459.
(45) Truong, N. D.; Galin, J. C.; François, J.; Pham, Q. T. *Polymer* **1986**, *27*, 467.
(46) Axelos, M. A. V.; Thibault, J. F.; Lefebvre, J. *Int. J. Biol. Macromol.* **1989**, *11*, 186.
(47) Axelos, M. A. V.; Thibault, J. F. *Int. J. Biol. Macromol.* **1991**, *13*, 77.
(48) Axelos, M. A. V.; Branger, M. *Food Hydrocolloids* **1993**, *7*, 91.
(49) Mackie, W.; Noy, R.; Sellen, D. B. *Biopolymers* **1980**, *19*, 1839.
(50) Martinsen, A.; Skjåk-Bræk, G.; Smidsørd, O.; Zanetti, F.; Paoletti, S. *Carbohydr. Polym.* **1991**, *15*, 171.
(51) Morawetz, H. In *Macromolecules in Solution*, 2nd ed.; Wiley: New York, 1975; p. 366.
(52) Westheimer, F. H.; Kirkwood, J. G. *J. Chem. Phys.* **1938**, *6*, 513.
(53) Westheimer, F. H.; Shookhoff, M. W. *J. Am. Chem. Soc.* **1939**, *61*, 555.
(54) Darvill, A.; Albersheim, P.; MacNeil, M.; Lau, J.; York, W.; Stevenson, T.; Thomas, J.; Doares, S.; Gollin, D.; Chelf, P.; Davis, K. *J. Cell Sci. Suppl.* **1985**, *2*, 203.
(55) Gacesa, P. *Carbohydr. Polym.* **1988**, *8*, 161.
(56) Smidsrød, O.; Glover, R. M.; Whittington, S. G. *Carbohydr. Res.* **1973**, *27*, 107.
(57) Smidsrød, O.; Haug, A. *Acta Chem. Scand.* **1968**, *22*, 797.
(58) Bouffar-Roupe, C. Ph.D., Grenoble, 1989.
(59) Axelos, M. A. V.; Mestdagh, M. M.; François, J. Results to be published.
(60) Morris, E. R.; Powell, D. A.; Gidley, M. J.; Rees, D. A. *J. Mol. Biol.* **1982**, *155*, 507.
(61) François, J.; Schwartz, T.; Weill, G. *Macromolecules* **1980**, *13*, 564.
(62) Axelos, M. A. V.; Mestdagh, M. M. To be published.
(63) Garnier, C.; Axelos, M. A. V.; Thibault, J. F. *Carbohydr. Res.* **1994**, *256*, 71.
(64) François, J.; Truong, N. D.; Medjahdi, G. *Eur. Polym. J.*, submitted for publication.
(65) Want, L.; Velings, N.; Mestdagh, M.; El Brahmi, K.; François, J. *Eur. Polym. J.*, submitted for publication.
(66) Stockmayer, W. H. *J. Chem. Phys.* **1943**, *11*, 45.
(67) Pezron, E.; Leibler, L.; Ricard, A.; Audebert, R. *Macromolecules* **1988**, *21*, 1126.
(68) de Gennes, P. G. *Scaling Concepts in Polymer Physics*; Cornell University Press: Ithaca, NY, 1979.
(69) de Gennes, P. G.; Pincus, P.; Velasco, R. M.; Brochard, F. *J. Phys. Paris* **1976**, *37*, 1461.
(70) Edwards, S. F. *Proc. Phys. Soc., London* **1966**, *88*, 265.
(71) Pfeuty, P. *J. Phys. Paris* **1978**, *39*, C2–149.